Effects of Climate and Land Cover Changes on Habitat for Herbivores at Mole National Park, Ghana

K. B. Dakwa

Department of Conservation Biology and Entomology, School of Biological Sciences, University of Cape Coast. Ghana

Corresponding Author: *dakb92@yahoo.com , kdakwa@ucc.edu.gh*

Abstract

The aim of this study was to determine climate and land cover changes in the MNP and the effect these could have on the large herbivores. Monthly temperature and rainfall data and Landsat satellite imagery from 1980 to 2013 for the Mole National Park (MNP) were acquired. Land cover classes of the imageries were validated through ground truth accuracy assessment procedure. Autoregressive integrated moving average (ARIMA) model was used to model the data using time series statistics with R. The results indicated a rise in temperature that became significant after two decades and a reduction in the amount of rainfall every decade. The decade mean temperature for the period 2000–2010 (2000s) reached the highest of 27.2 ± 0.15 ºC while the 1980s recorded the least of 26.7 ± 0.25 ºC. The decade mean rainfall for the 1980s reached the highest of 129 ± 9.91 mm while the least of 93.9 ± 7.41 mm was recorded in the 2000s. There was a strong and significant negative correlation between the mean rainfall time series and the mean temperature time series for the period under review. The shrub-land occupied the largest part of the Park (about 26%) followed by the open savanna (23%). Rainfall influenced the open savanna, grass and shrub classes immediately, but the closed savanna lagged behind rainfall by five years. As forecast suggested a relatively high temperature and low rainfall, the shrub-land and grassland are likely to shrink while open and closed savanna woodland areas expand by 2020. Accordingly, there may be shrinking forage resources for the grazers and abundant forage for the browsers during the period. It is recommended to reduce the extent of burning at MNP during the forecast period to make forage sufficiently available for grazing. Regular follow up to this study could provide a guideline to securing habitats, and forage, for MNP's herbivores.

Introduction

Protected areas (PAs) are the safest places for most large mammal populations in Africa (Dakwa, Monney, & Attuquayefio, 2016; Dakwa, Monney, & Attuquayefio, 2014; Barnes, 1999; Newmark, 1996) but their populations continue to decline because of the changes, mainly due to environmental and anthropogenic activities, that influence ecological processes within the PAs (Bartlam-Brooks, Bonyongo, & Harris, 2013). The most important global environmental changes that affect PAs are land cover and climate changes (Turner & Meyer, 1994). Climate change has resulted in an imbalance between the flora and fauna that characterize tropical savanna communities (Rustad et al., 2001). Failure to understand how climate influences land cover change processes limits the ability to manage PAs (Bartlam-Brooks et al., 2013; Serneels, Said, & Lambin, 2001).

Remote sensing is a popular application for land cover change detection studies (Lambin, Geist, & Lepers, 2003). It provides quantitative and spatial datasets for land cover change analysis and interpretation. Geographic Information Systems (GIS) is applied to remotely sensed data to generate maps and statistical estimates for modeling and monitoring changes detected (Woodwell et al., 1984; Dakwa, 2016a). Landsat satellite imagery is one of the tools used for mapping and monitoring land cover changes and its association with ground-truth surveys facilitates accuracy assessment for classified satellite imagery (Congalton, 1996). Change detection is important for the management of PAs, as this provides information on change dynamics of the

vegetation of the area, which could be a useful indication of the effect this could have on the population of wildlife. Despite these, there are no quantitative data for change detection at MNP. Wildlife research in MNP is scanty in general including evaluation of population trends and status of lions (Burton et al., 2010), cost of wildlife raids (Dakwa, 2016b), allometry in sympatric grazers (Dakwa, 2016c) and a number of community and wildlife conflict issues which remain unpublished. The aim of this study was to determine climate and land cover changes in the MNP over a 30-year period, forecast changes in the next seven years, determine the effects of such changes on the large herbivores and predict the effects such changes could have on the herbivores over the forecast period.

Materials and Methods

Study area

The Mole National Park (Figure 1) lying between 9° 11" and 10° 10" N and between 1° 22" and 2° 13" W covers an area of about 4,840 km² and it is located in northwest Ghana on grassland savanna and riparian ecosystems (Wildlife Division, 2011). This area of Ghana receives an average of 1,100 mm per year of rainfall (Wildlife Division, 2011). There are few main habitat types including riverine, swamp, closed savanna woodland and open savanna woodland but the open savanna woodland is the dominant habitat type (Schmitt & Adu-Nsiah, 1993). The Park is home to over 93 mammal species including the savanna elephant (*Loxodonta africana africana*) and buffalo (*Syncerus caffer*). The park is bordered by 33 communities, with a total estimated population of about 35,000 (Dakwa, 2016b).

Data collection

Acquisition of climate, land cover and vegetation data

Monthly temperature and rainfall data for the MNP from 1980 to 2013 were acquired from the Bole-Bamboi District Meteorological Office, which monitors the rainfall and temperature patterns from their station at the reserve's headquarters. ESRI license was provided by the University of Bristol to produce Landsat satellite imagery (Landsat ETM + at 30-m
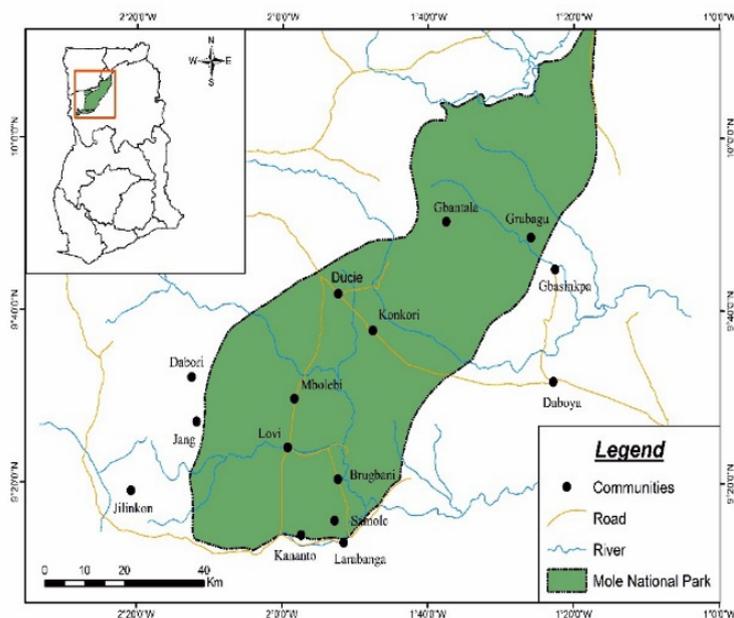

Figure 1 Map of Mole National Park. Source: Adopted from Dakwa (2016d)

spatial resolution) in the unsupervised mode for 1980, 1985, 1990, 1995, 2000, 2005, 2010 and 2013.

Ground truth accuracy assessment of land cover classes

Each of six groups of field assistants worked within one sixth portion of the park from August to December, 2013, to verify whether the unsupervised land cover classes assigned by the remote sensing was the same as observed on the field.

Coordinates of randomly chosen pixels picked out from the 2013 satellite image were located by the help of compasses and Garmin eTrex 10 Worldwide GPS Handled Navigators (all Garmin Ltd., Olathe, KA, USA). Field sites, 200 m x 200 m each, were then demarcated using existing landmarks and dimensions mapped out using a rangefinder (Yardage Pro Compact 800, Bushnell factory, Overland, KA, USA) for ground truth assessment. The land cover classes obtained from classified images in the unsupervised mode by the remote sensing software were (i) closed savanna woodland, (ii) open savanna woodland, (iii) shrub/dense herbaceous, (iv) grass/herbaceous, and (v) bare/built-up area (Table 1).

Obtaining ground truth point data from a wide geographic distribution throughout the study area would ensure that adequate point data were collected for all land cover classes of the satellite images.

This would involve a large number of samples for all land cover classes, which was difficult, logistically, and not practical for the entire study area. According to Congalton (1996), collecting a minimum of 50 samples for use in an error matrix is a good rule of thumb, however, fewer data points were envisaged for some of the land cover classes due to the difficulty of locating about 50 field sites, each of 200 x 200 m dimensions, for each class at various places in the park. To compensate for this, smaller plots of 30 x 30 m were randomly sampled at six to nine different locations in each of all the field sites (Table 2) and every effort was made to collect additional data from 30 m x 30 m field sites, independently of the 200 x 200 m, for those classes. It was assumed that replicates in any field site were considered separate data points for scoring in the accuracy

TABLE 1
Description of Land Cover Classes

Land cover class	Description
Closed savanna woodland	Savanna vegetation dominated by woody plants, mostly trees, which are close to each other and often forming canopies that shade the vegetation floor from sunlight.
Open savanna woodland	Savanna vegetation with admixture of woody plants, mostly trees, and herbaceous plants. Trees dominating the vegetation somehow but are well spaced, forming few or no canopies and therefore admitting enough sunlight at the vegetation floor.
Shrub / dense herbaceous	Shrubs interspersed with a mixture of largely dense herbaceous plants with little wood and few dense herbaceous plants with no wood.
Grass / herbaceous	Mostly grasses interspersed with few other herbaceous plants.
Bare / built-up area	Bare area without vegetation, including water bodies, buildings, rocky surfaces and roads.

Source: Wildlife Division (2011)

assessment. Altogether 300 samples, 60 for each class (Table 2), were assessed. Following the pixels of satellite images, each field site was located at ten different places for open savanna and grass, seven different places for closed savanna and shrub/dense herbaceous, and six for bare/built-up. A 30 x 30 m plot was surveyed randomly six times within field sites for each of open savanna and grass classes, seven times for closed savanna and shrub/dense herbaceous, and nine times for built-up. In addition, a 30 x 30 m field site was traced and located for closed savanna at 11 places; shrubs, 11 places and; bare/built-up, six places (Table 2).The number of times a class on the field was the same or different from the one obtained in the unsupervised mode were recorded.

Data analysis

Rainfall, temperature and land cover changes data over a period spanning 1980-2013 were analysed using time series statistics with R (R Core Team, 2014) to establish the relationships among them, to model them with an autoregressive integrated moving average (ARIMA explain the model) model, and forecast next observations in the time series as it was possible. The *xts* package (Ryan & Ulrich, 2014) was used for the time series data representation because it is versatile enough for time series data structure. However, the package *st series* (Trapletti & Hornik, 2015) and *forecast* (Hyndman, 2015; Hyndman & Khandakar, 2008) were also used for their appropriate analyses as was necessary. Autocorrelations and partial autocorrelations were calculated using the autocorrelation function (*ACF*) and partial autocorrelation function (*PACF*) respectively from the *xts* package. The presence of autocorrelations is one step forward in the time series analysis as it indicates that an ARIMA model could model the time series.

The ARIMA model includes the model order, *p, d, q,* which represent the number of autoregression (AR) coefficients, the order of differencing and the number of moving average (MA) coefficients respectively and it begins with the determination of d, which is needed to make the series stationary. At the lowest order of differencing the time series is expected to fluctuate around a certain mean value and its *ACF* plot approaches zero rapidly. From the number of significant autocorrelations in the *ACF* output q was estimated, and from the *PACF* output, p was estimated. The cross-correlation function (CCF) was used to deduce the presence of lagged correlations between mean rainfall time series and mean temperature time series; mean rainfall time series and land cover changes time series, between time series of land cover variables etc. over the time frame. Also, the Ljung–Box test function

TABLE 2
Sampling Details for Ground Truth Accuracy Assessment for each Class

Quadrats at field sites	Classes				
	Open savanna	Closed savanna	Shrub	Grass	Bare/ built-up
Number of 200 m x 200 m	10	7	7	10	6
(No. of replicates of plots at field site)	(6)	(7)	(7)	(6)	(9)
No. of additional 30 m x 30 m	-	11	11	-	6
Total no. of 30 m x 30 m sample plots	60	60	60	60	60

from the *xts* package, which implements the Box–Pierce statistical test was used to test the time series for the presence or absence of autocorrelation (or partial autocorrelation) when samples are small (Box & Pierce, 1970; Ljung & Box, 1978; Harvey, 1993). Forecast by ARIMA modelling has three stages: model identification (fitness), parameter estimation, and diagnostic checking, which run repeatedly to obtain a model that suits the given data for time series prediction. The ARIMA model was fitted to the rainfall and temperature time series data using the *arima* function in the *forecast* package to estimate the coefficients, standard errors and confidence intervals. After validating the ARIMA model, the *predict* function was used in the forecast package to *forecast* the observations for the annual mean rainfall and annual mean temperature time series in the next seven years (up to 2020). As it was necessary to test whether the mean rainfall or the mean temperature time series was mean reversible or random walk, the Augmented Dickey−Fuller (ADF) test (Said & Dickey, 1984) was used, which is implemented by the *adf.test* function of the *tseries* package. From the output of the Dickey–Fuller test one can ascertain the presence or otherwise of a unit root in an autoregressive (AR) model. When a unit root is present the model would be non-stationary (Dickey & Fuller, 1979; Said & Dickey, 1984).

Results

Rainfall and temperature time series.
The decade mean temperature for 2000–2010 was the highest (27.2 ± 0.15 0C; range = 24.7-31.5 ^{0}C) followed by 1990–1999 with 27.1 ± 0.15 ^{0}C (range = 24.4-31 ^{0}C) and the least was 26.7 ± 0.25 0C (range = 24.3-32.7 ^{0}C) in 1980-1989. Results of ANOVA revealed the differences in the three decade

mean temperatures were significant, $F_{(2, 360)} = 3.49$, $\rho < 0.05$, but Tukey's post-hoc analysis indicated the differences were only significant between the 1980s and 2000s (Tukey's pairwise = 3.58, $\rho < 0.05$). The decade mean of rainfall for the 1980s was the highest (129 mm ± 9.91 mm, range = 0-362 mm) followed by the 1990s with 95.9 mm ± 10.17 mm (range = 0–390.4 mm) and the least of 93.9 mm ± 7.41 mm (range = 0-304.1 mm) in the 2000s. ANOVA results indicated the differences in the three decade mean rainfall values were significant, $F_{(2, 357)} = 4.54$, $\rho < 0.05$; Tukey's post-hoc analysis indicated significant differences between the 1980s and 1990s (Tukey's pairwise = 3.58, $\rho < 0.05$) and between 1980s and 2000s (Tukey's pairwise = 0.99, $\rho < 0.05$).

Figure 2 shows the trends of changes between the temperature time series and the rainfall time series. There was a negative correlation (r = -0.511) between the mean rainfall time series and the mean temperature time series for the period under review. The estimated value from the series' cross-correlation function (CCF) revealed the relationship between the trends of changes of mean rainfall and mean temperature was significant (Figure 3), meaning that when the mean rainfall decreased,
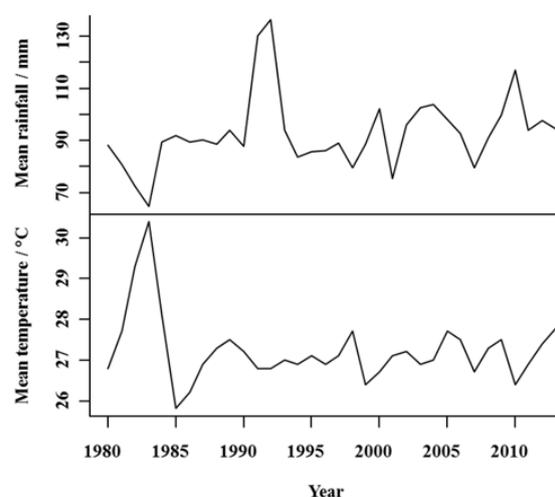

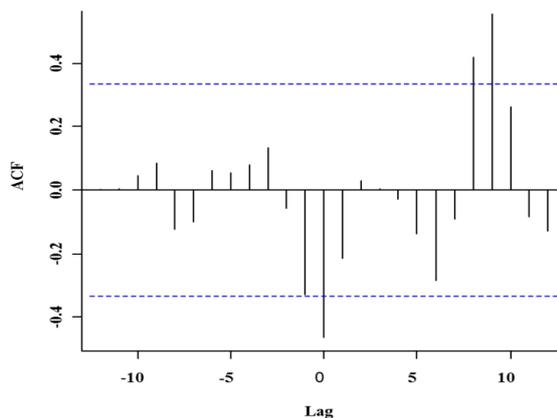Figure 2: Trends of changes of mean rainfall (mm) and mean temperature (0C) from 1980 – 2013 at MNP

Figure 3: Cross correlation function between mean rainfall and mean temperature time series from 1980 – 2013 showing correlations are significant at lags 8 and 9

the mean temperature rose and when the mean rainfall rose, the mean temperature decreased.

Furthermore, Box-Ljung test confirmed the suitability of both the mean rainfall time series (χ^2 = 6.95, df = 1, ρ-value = 0.008) and the mean temperature time series (χ^2 = 9.14, df = 1, ρ-value = 0.002) for time series analysis. The autocorrelation function (ACF) for mean rainfall time series (Figure 4) indicated one MA and this suggested that its ARIMA model would require one MA coefficient, {MA(1); thus, q in the model order = 1. The time series partial ACF (Figure 5) showed there was one lag value that was statistically significant so the initial model would have one AR coefficient, {AR(1)}; thus p in the model order = 1. The *difference* function revealed zero difference and this suggested that d in the model order is 0. The model assumed that the original series was stationary (mean-reverting, Dickey-Fuller = -3.0473, Lag order = 3, ρ = 0.017). As the ACF and the partial ACF results (Figures 4 and 5, respectively) were a little difficult to interpret, *auto.arima* function confirmed the best order for (*p, d, q*) in the ARIMA model as (1, 0, 1). The mean rainfall data series fitted the model because the *tsdiag*
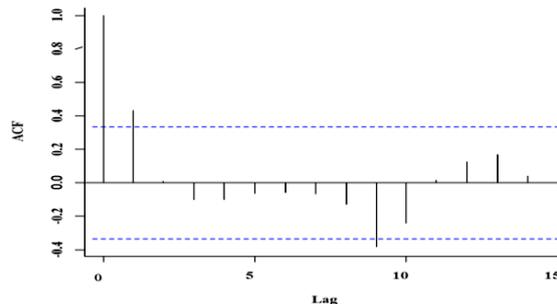

Figure 4: Autocorrelation of mean rainfall time series from 1980–2013 showing it is significant at lag 9 which crosses the dash line as lag 1 is too close to zero
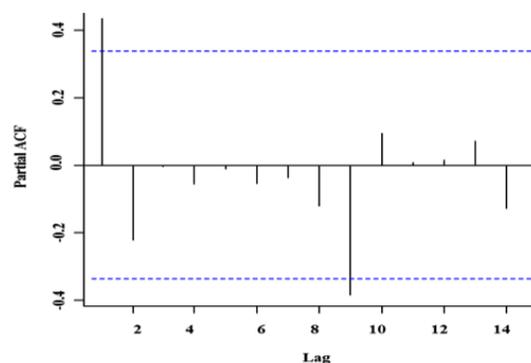

Figure 5: Partial autocorrelation of mean rainfall time series from 1980-2013 showing it is significant at lag 9 which crosses the dash line as lag 1 is too close to zero

function for model diagnostics, fitness and validation indicated standardized residuals did not show clusters of volatility (Figure 6), the autocorrelation function (ACF) showed no significant autocorrelation between the residuals (Figure 6), and the *p*-values for the Ljung–Box statistics were all large (Figure 6), indicating that the residuals were patternless. In the same way as the mean rainfall time series, the best order for (*p, d, q*) in the ARIMA model for the mean temperature time series was (2, 0, 0) and this was confirmed by the *auto.arima* function. The mean temperature data series also fitted the model.

Forecasting
Figure 7 shows the results of a forty-year trend of changes between rainfall and temperature (from 1980 to 2020) including a seven-year
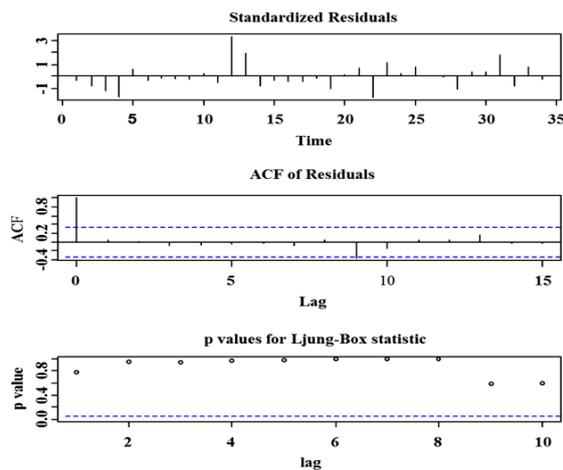
Figure 6: Graphical results of model diagnostics by Ljung–Box statistics of the ARIMA model for mean rainfall time series showing the model is a good fit
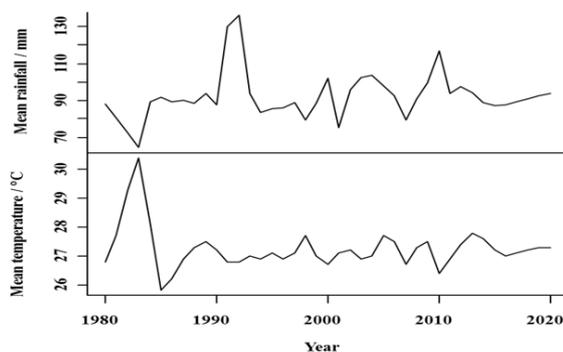

Figure 7: Mean rainfall and mean temperature over 40 years including forecast period up to 2020

forecast period from 2013 to 2020. While the mean annual rainfall is expected to remain low over the period between 2013 and 2020, the mean annual temperature is expected to remain high. Thus, the mean annual rainfall will possibly rise and the mean annual temperature reduce in future as expected of time series that were mean reverting.

Imagery, matrices of land cover and ground truth accuracy assessment

Figures 8 and 9 show Landsat satellite imageries for the years 1980, 1985, 1990, 1995; and 2000, 2005, 2010, 2013 respectively. Table 3 shows the matrices of land cover by class values for the years 1980, 1985, 1990,

1995, 2000, 2005, 2010 and 2013 obtained from Landsat satellite imageries; and Table 4 displays results of ground truth accuracy assessment of the 2013 imagery. An overall accuracy of 80.3% and class accuracy ranging from 71.67–88.33% (Table 4) were high enough to validate the imagery. Therefore the matrix of land cover by class values (Table 3) were reasonable estimates of land occupancy by the various land cover classes in the MNP. Analysis of variance (ANOVA) indicated very highly significant difference among the various land cover classes ($F_{(4, 35)} = 29.358$, $\rho < 0.001$), and Tukey's *post hoc* analysis indicated that there was a very highly significant difference between six out of the 10 pairs of the five different land cover classes. Only pairs including bare/built-up area were not significant. The shrub/herbaceous class occupied the largest part of the Park (1,261 km^2), constituting 26% of the park's total area (Table 3), followed by the open savanna, with an average of 1,111 km^2 (23% of the park's area) and the built-up with an average of 629 km2 occupied the least area of 13% (Table 3).

Land cover time series

None of the five land cover class time series correlated with the other as the CCFs of all 10 pairs were not significant, therefore, ARIMA models could not be used to model the land cover class values as a time series. Neither rainfall time series nor temperature time series cross-correlated with any of the land cover class values time series. However, there appeared to be a clear and consistent trend of land cover changes with rainfall over the years (Figure 10). For example, a decrease in the amount of rainfall from 1980 to 1990 corresponded with an increase in the expanse of shrubs/herbaceous and grass/herbaceous
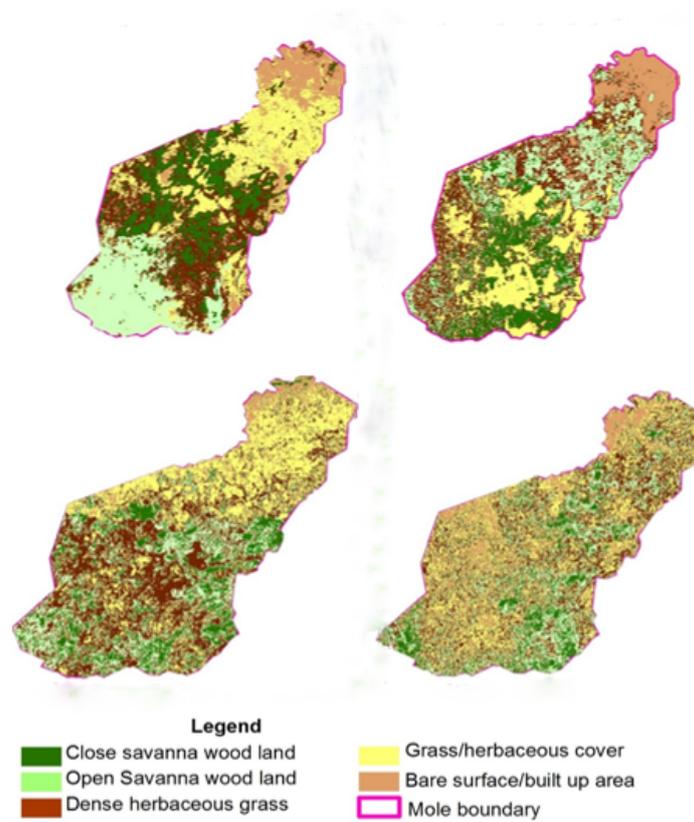
Legend

■	Close savanna wood land	■	Grass/herbaceous cover
■	Open Savanna wood land	■	Bare surface/built up area
■	Dense herbaceous grass	▢	Mole boundary

Figure 8: Landsat satellite images for the years 1980 (top left), 1985 (top right), 1990(bottom left) and 1995 (bottom right)

Legend

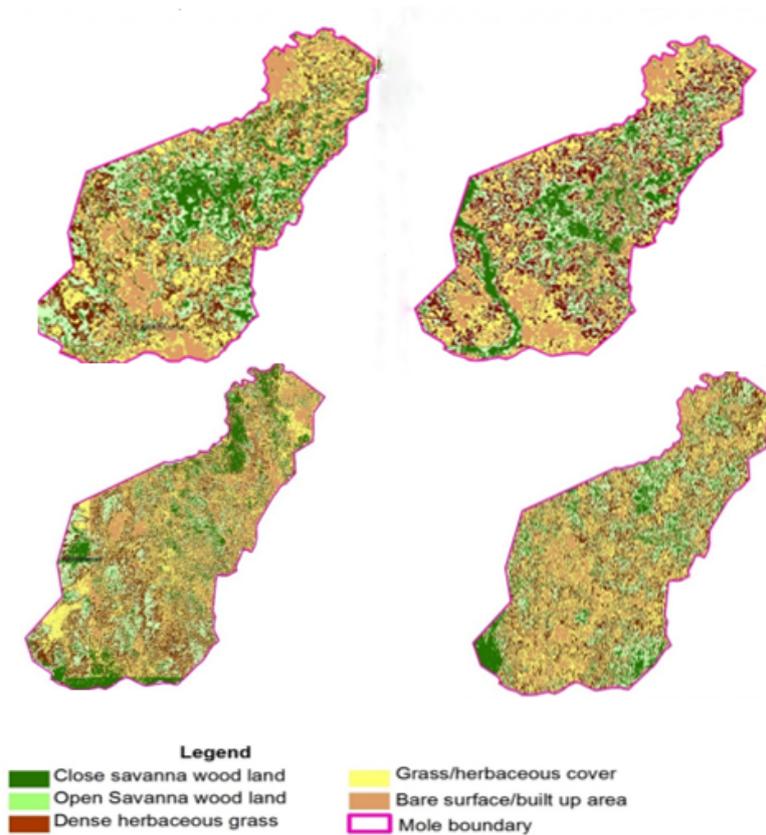|			
■	Close savanna wood land	■	Grass/herbaceous cover
■	Open Savanna wood land	■	Bare surface/built up area
■	Dense herbaceous grass	▢	Mole boundary

Figure 9: Landsat satellite images for the years 2000 (top left), 2005 (top right), 2010 (bottom left) and 2013 (bottom right)

TABLE 3

Year	Class value (sq. km)				
	Closed savanna woodland	Open savanna woodland	Dense shrubs / herbaceous	Grass / herbaceous	Bare / built-up area
1980	959	1098	1124	1031	628
1985	889	1046	1191	1074	640
1990	688	996	1587	1301	267
1995	592	1211	1454	926	657
2000	791	1192	1006	1103	747
2005	773	1123	1169	1032	742
2010	698	1020	1353	1145	623
2013	566	1203	1205	1141	724
Average	744	1111	1261	1094	629

Matrix of Land Cover by Class Values based on Landsat Images to the nearest sq. km

TABLE 4

Class	Closed savanna woodland	Open savanna woodland	Dense shrubs / herbaceous	Grass / herbaceous	Bare / built-up areas
Closed savanna woodland	52	8	0	0	0
Open savanna woodland	6	44	5	5	0
Shrub/herbaceous	1	3	49	7	0
Grass/herbaceous	1	5	4	43	7
Bare/ built-up areas	0	0	2	5	53
Sum	60	60	60	60	60
Class accuracy (%)	86.67	73.33	81.67	71.67	88.33
Overall accuracy (%)	80.33				

Ground Truth Data Assessing the 2010 Landsat Satellite Image in 2012/2013

and, while the amount of rainfall increased for the next five years to 1995, the expanse of shrubs/herbaceous and grass/herbaceous classes reduced correspondingly. From 2000 to 2010, rainfall pattern was up and down and so the extent of grass cover went down and up respectively. There was also a corresponding increase in the expanse of closed savanna class with the amount of rainfall from 1980 to 2000. There appeared to be a similar trend in the pattern of rainfall with the expanse of the closed savanna class, both rising between 1980 and 2000, with the exception that the closed savanna tended to be lagging behind the amount of rainfall for five years. Thereafter, the trend changed and a rise in the amount of rainfall corresponded with a decrease in the expanse of the closed savanna class.

The relationships between temperature and the land cover classes were as clear as they were between rainfall and the land cover classes with temperature affecting the land cover classes in the opposite way to rainfall (Figure 10). In general, there appeared to be a trend of change between the amount of rainfall and the expanse of all the land cover classes from 1980 to 1995 and in all cases but the closed savanna class, the trough or peak of the trend occurred in 1990, while trends after 1995 were not consistent. These trends suggest that the amount of rainfall influenced the open savanna, grass/herbaceous and shrub/herbaceous classes immediately, while the lag phase in the case of the closed savanna was expected for an area that had dense tree cover as it takes longer for trees to respond to changes.

As forecast suggested a relatively low rainfall from 2010 to 2020, the land cover sizes of shrub-land and grassland are expected to reduce and the sizes of closed and open savanna classes expected to increase correspondingly.

The interclass trends also show some consistent relations were between closed savanna and open savanna and between shrub/herbaceous and grass/herbaceous, and somewhat inverse relations between grass/herbaceous and bare classes (Figure 10). Closed savanna lagged behind open savanna but they appeared to show positive relationship.

Discussion

The use of Landsat satellite imagery in change detection is limited by the effect of weather and other obstacles that interfere with the output of these passive sensors. Despite these limitations, ecological application of Landsat satellite is still widely used by researchers to monitor land cover and land use changes. The results indicated a high and valid ground truth accuracy for the interpretation of the imagery. The 19.7% error in this study implied that the Landsat satellite output was not perfect, but this was to be expected.

The results indicated a rise in temperature that became significant after two decades and a reduction in the amount of rainfall every decade. There seemed to be an inverse relationship between temperature and rainfall in the MNP so that when there was a high mean temperature, there was a correspondingly low mean rainfall and *vice versa*. The effect
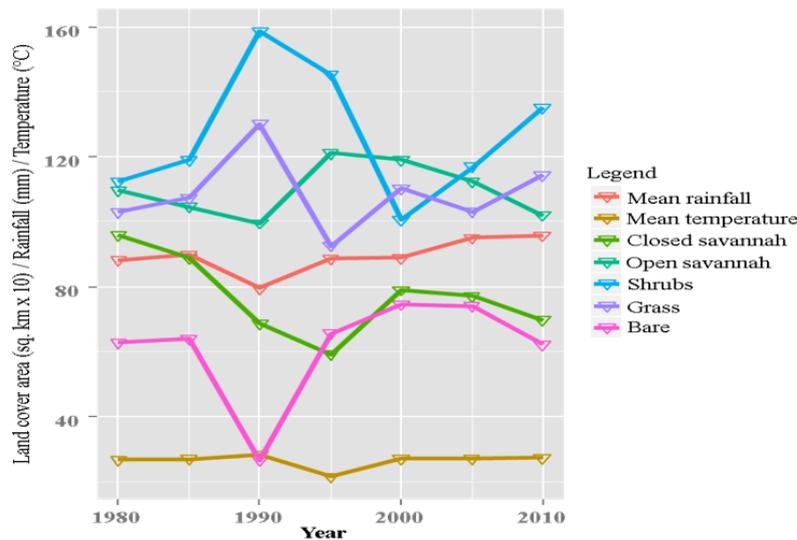

Figure 10: Land cover changes with rainfall and temperature

of rainfall on the MNP ecosystem cannot be over-emphasized. For example, the ability of trees and grasses to make good use of soil moisture, is primarily determined by rainfall (Scholes & Archer, 1997). While the effect of rainfall on grass at MNP was immediate, there was a time lag in the case of trees. Thus, in terms of forage, there was a correspondingly immediate benefit of rainfall to the large grazers. Primary productivity depended largely on rainfall and so forage quality and quantity varied seasonally as noted by Dakwa (2016d) and both reached a peak during the flood season, with a sharp decline to the trough in the fire season (Dakwa, 2016d). Seasonal rainfall can refill ephemeral water sources, triggering the assemblages of large numbers of grazer species in such areas that were otherwise unselected during the dry season (Western, 1975; Dakwa, 2016d). Temperature followed a similar pattern inversely, though with narrow variations, so that seasonal effects of temperature resulted in drying of most water sources that compelled large numbers of grazers to concentrate around few water holes in MNP (Dakwa, 2016d). Forecasts for the next seven years suggested a continuum of slight increases in mean rainfall following a four-year sharp drop in annual mean rainfall at MNP. This is an indication that between 2010 and 2020 shrub-land and grassland are likely to shrink while open and closed savanna woodland areas expand at MNP. Accordingly, there will be shrinking forage resources for the grazers and abundant forage for the browsers during the period.

In conclusion, there has been climate change over the past 30 years, from 1980, at MNP and this resulted in land cover changes, though other factors including fire played a part in the land cover changes. The changes to land cover of MNP affected large grazers in ways related to their habitat and forage resource requirements. It is projected that land cover changes would result in abundant forage for browsers and shrinking forage for the grazers at MNP in the later years up to 2020. It is recommended to reduce the extent of burning at MNP during the period to make forage sufficiently available for grazing. Regular follow up to this study could provide a guideline to securing habitats, and forage, for MNP's herbivores.

References

Barnes, R. F. W. (1999). "Is there a future for elephants in West Africa?" *Mammal Review* **29**:175-200.

Bartlam-Brooks, H. L. A, Bonyongo M. C., and Harris, S. (2013). How landscape scale changes affect ecological processes in conservation areas: external factors influence land use by zebra (*Equus burchelli*) in the Okavango Delta. *Ecology and Evolution* **3**, 2795–2805

Box, G. E. P., and Pierce, D. A. (1970). Distribution of residual correlations in autoregressive-integrated moving average time series models. *Journal of the American Statistical Association*, **65**:1509–1526.

Burton, A. C., Buedi, E. B., Balangtaa, C., Kpelle, D. G., Sam, M. K. and Brashares, J. S. (2010) The decline of lions in Ghana's Mole National Park. *African Journal of Ecology*.**49**:122–126.

Congalton, R. G. (1996). Accuracy assessment: a critical component of land cover mapping. *Journal of Landscape Ecology*. **14:** 119-131.

Dakwa, K. B. (2016a). Monitoring and evaluation of vertebrate fauna composition and structure of a high forest zone in Ghana,

20 years after heavy logging. *Journal of Biology and Nature*. 5(4): 196-210.

Dakwa, K. B. (2016b). How does the cost of raid influence tolerance and support of local communities for a wildlife reserve? *International Journal of Biodiversity and Conservation*. 8(4): 81-92.

Dakwa K. B. (2016c). Allometry in sympatric grazers: Does it influence their abundance, distribution and resource selection and use patterns in the Mole National Park? *Journal of Biology and Nature*. 5(4): 177-184.

Dakwa, K. B. (2016d). *Effects of environmental changes on the assemblages of eight sympatric large grazers in the Mole National Park, Ghana.* Unpublished doctoral thesis. University of Cape Coast, Cape Coast, Ghana.

Dakwa, K. B., K. A. Monney, and D. Attuquayefio. (2014). Density and distribution of bongos (*Tragelaphus eurycerus*) in a high forest zone in Ghana. *Journal of Ecology and the Natural Environment,* 6(9): 331-341.

Dakwa, K. B., K. A. Monney, and D. Attuquayefio. (2016). Raid range selection by elephants around Kakum Conservation Area: Implications for the identification of suitable mitigating measures. *International Journal of Biodiversity and Conservation,* 8(2): 21-31.

Dickey, D. A. and Fuller, W. A. (1979). Distribution of the Estimators for Autoregressive Time Series with a Unit Root. *Journal of the American Statistical Association*, 74; 427–431.

Harvey, A. C. (1993) *Time Series Models.* (2nd ed.). Wheatsheaf, NY: Harvester.

Hyndman, R. J. (2015). _forecast: Forecasting functions for time series and linear models. R package version 6.1. Retrieved from http://gitub.com/dn/f-cast.

Hyndman, R. J., and Khandakar, Y. (2008). Automatic time series forecasting: the forecast package for R. *Journal of Statistical Software*, 26(3); 1-22. .

Lambin, E. F., Geist, H. J., and Lepers, E. (2003). Dynamics of land-use and land-cover change in tropical regions. Annual review of environment and resources, 28(1): 205-241.

Ljung, G. M., and Box, G. E. P. (1978). On a measure of lack of fit in time series models. *Biometrika*, **65**: 297–303.

Newmark, W. D. (1996). Insularization of Tanzanian parks and local extinction of large mammals. *Conservation Biology* 10: 1549–1556

R Development Core Team (2014). *R: A language and environment for statistical computing.* Vienna, Austria:R-Foundation.

Rustad, L. E. J. L., Campbell, J., Marion, G., Norby, R., Mitchell, M., Hartley, A. and Gurevitch, J. (2001). A meta-analysis of the response of soil respiration, net nitrogen mineralization, and aboveground plant growth to experimental ecosystem warming, Oecologia. **126**(4): 543-562.

Ryan, J. A., and Ulrich, J. M. (2014). xts: extensible Time Series. R package version 0.9-7. Retrieved from http://CRAN.R-project.org/package=xts.

Said, S. E. and Dickey D. A. (1984). Testing for Unit Roots in Autoregressive-Moving Average Models of Unknown Order. *Biometrika*, 71: 599–607.

Schmitt, K. and Adu-Nsiah M. (1993) *The Vegetation of Mole National Park. (Forest Resource Management Project Report No. 14).* Accra, Ghana: Wildlife Division.

Scholes, R.J., and Archer, S. R. (1997). Tree-grass interactions in savannas. Annual

Review of Ecology and Systematics. **28**: 517-544.

Serneels, S., Said, M. Y. and Lambin, E. F. (2001). Landcover changes around a major east African wildlife reserve: the Mara Ecosystem (Kenya). *International Journal of Remote Sensing.* **22**: 3397–3420.

Trapletti, A. and Hornik, K. (2015). tseries: Time Series Analysis and Computational Finance. R package version 0.10-34. Retrieved from http://CRAN.R-project.org/ package=tseries.

Turner, B. L., and Meyer, B. L. (1994). Global land use and land cover change: an overview. In W. B. & Meyer, B. L. Turner (Eds.), *Changes in Land Use and Land Cover: A Global Perspective* (pp.3-10). Cambridge, UK: Cambridge University Press.

Western, D. (1975). Water availability and its influence on the structure and dynamics of a savanna large mammal community. *African Journal of Ecology.* 13: 265-286.

Wildlife Division (2011). *The Management Plan of Mole National Park.* Accra, Ghana: Wildlife Division Support Project.

Woodwell, G., Hobbie, J. E., Houghton, R. A., Melillo, J. M., Moore, B., Park, A. B. and Shaver, G. R. (1984). Measurement of changes in the vegetation of the earth by satellite imagery. *The role of terrestrial vegetation in the global carbon cycle: measurement by remote sensing SCOPE*, **23**: 221-240.